Research Article

World Journal of Pharmaceutical and Life Sciences
WJPLS

SPECTROSCOPIC CHARACTERIZATION FOR ADSORPTION PROCESSES OF CADMIUM IONS (cd^{+2}) ONTO ZEOLITE-A TREATED BY COLD PLASMA

Magdy A. Wassel*[1], Hoda. A. Bayoumi, Anwer A. Wassel[3], Ahmed S. Elzaref[1] and Mahmoud M. Arafa[4]

[1]Chemistry Department, Faculty of Science, Al-Azhar University, Cairo, Egypt.
[2]Chemistry Department, Women's College for Art Science and Education, Ain Shams University, Cairo, Egypt.
[3]Imam Abd El-Rhman Bin Fesal University, College of Science, Chemistry Department, Damam, KSA.
[4]Department of Chemistry, Faculty of Science, El-Menoufia University, Shebin El-Kom, Egypt.

*Corresponding Author: Magdy A. Wassel

Chemistry Department, Faculty of Science, Al-Azhar University, Cairo, Egypt.

ABSTRACT

In this manuscript, we have studies the spectroscopic characterization (FTIR-ATR, X-ray diffraction and SEM-EDS analysis) for adsorption processes of cadmium ions (Cd^{+2}) onto zeolite-A treated by cold plasma and effect of different flow rate of oxygen gas and cold plasma time before and after the adsorption by zeolite-A and zeolite-A treated by cold plasma.

KEYWORDS: spectroscopic, Zeolite-A, Cold plasma, adsorption, Cadmium ions.

INTRODUCTION

Synthetic zeolites have many advantages in water purification so it is called scavenger of hazardous and toxic metals. Furthermore, it has the potential in effluent treatment for removal of dyes and heavy metals and for applications such as permeable reactive barriers and contaminant barrier liners. The contaminant removal using zeolites takes place through adsorption and/or precipitation and the removal efficiency depends upon the pH, initial contaminant concentration and the solid to liquid ratio of the system. Bacterial loading on fly ash based zeolites can be used for heavy metal and phosphate removal, thus offering, an economically viable alternative to existing methods.[1]

Many types of zeolites have been developed based on kaolinite in previous years. In the hydrothermal synthesis of kaolinite based zeolites, aging for 48 h at room temperature is suitable for various types of zeolites and metakaolinization at 600 to 700°C, where the period of 2 h. is enough to transform the kaolinite into an amorphous state. However, there are several crucial factors that need to be considered to produce specific zeolites Low Si/Al molar ratio (Si/Al ≤ 5), various types of LTA and X zeolites.[2]

Additionally, zeolite-A is the universal type of synthetic zeolite in the area of detergent and water softening, due to its large ion exchange capacity, mechanical strength and particular crystal shape. Besides, it is environmentally safe with almost zero loading of harmful effect on the environment.[3]

The structures of zeolites consist of three-dimensional frameworks of SiO_4 and AlO_4 tetrahedra. The aluminum ion is small enough to occupy the position in the center of the tetrahedron of four oxygen atoms, and the isomorphous replacement of Si^{+4} by Al^{+3} produces a negative charge in the lattice.[4] The net negative charge is balanced by the exchangeable cation (sodium, potassium or calcium). These cations are exchangeable with certain cations in solutions such as lead, cadmium, zinc, and manganese. The fact that zeolite exchangeable ions are relatively innocuous (sodium, calcium, and potassium ions) makes them particularly suitable for removing undesirable heavy metal ions from industrial effluent waters. One of the earliest applications of a natural zeolite was in removal and purification of cesium and strontium radioisotopes.[4]

Different types of zeolites have been used for adsorption of heavy metals and waste water treatment. A large proportion of these literatures contained results of batch experiments for the following parameters; contact times, pH, metal concentrations, metal/adsorbent mass ratio. In these studies, many authors reported the successful removal of copper, zinc, nickel, cadmium, cobalt and lead. All these zeolites are known to have basically these two main components; SiO_2 and Al_2O_3 but their proportions vary. These are also the two main components of zeolite-A and therefore we can prepare from Egyptian kaolin.

zeolite-A is one of the studies were used for removing toxic metals from a wastewater. The ability of zeolite-A to remove metal cations from wastewater has been demonstrated in many literatures.[5]

Zeolite-A is synthesized using natural kaolin from Ethiopia. Raw kaolin and mechanically purified kaolin from Ansho, southern part of Ethiopia, have been surveyed. The starting kaolin and the final zeolite-A samples were characterized by X- Ray Diffraction (XRD), elemental analysis (ICP), Scanning Electron Microscopy (SEM), Thermogravimetric Analysis (TGA) and Cation Exchange Capacity (CEC). Metakaolinization was achieved by calcining the kaolin in air at $600^{\circ}C$ within 3 hours. The optimization of the hydrothermal synthesis includes various NaOH concentrations at $100^{\circ}C$, for different reaction time. zeolite-A with molar ratio $SiO_2/ Al_2O_3 = 2.04$ and $Na_2O/SiO_2 = 0.44$ was obtained with 90% crystallinity using solid/liquid (1.25 g/25 ml) and reaction time of 3 h which is significantly lower than another method value that can reach up to 24 hours. Cubic crystal with rounded edge of zeolite-A having cation exchange capacity of 295 mg $CaCO_3$/g (4.6 meq Ca^{+2}/g) of anhydrous zeolite is obtained that can be a good candidate for detergent formulation.[3]

The use of plasma for surface modifications is a good alternative to classical organic chemistry reactions. These kinds of modifications are relatively easy and quick, without any toxic chemicals, and under soft plasma conditions the ablation of material is negligible. The plasma can be used to formation various functional groups onto the surface. plasma functionalization occur by using gases like O_2, N_2, CO_2, CF_4, He, Ar plasma induce the attachment of polar or non-polar functional groups like hydroxyl, carbonyl (with O_2, CO_2), amine (with N_2) and fluorinated groups (with CF_4) to the surface. The interactions of such surfaces with a specific surrounding environment are modified.[6]

Cold plasma (CPTAS), formaldehyde (FTAS), and microwave radiation treated (MTAS) acorn shell obtained from Quercus petraea tree as biosorbent was characterized and its dye removal ability at different dye concentrations. The isoelectric point, functional groups and morphology of acorn shell was investigated as adsorbent surface characteristics. Fourier transform infrared (FTIR), scanning electron microscopy (SEM), and UV–Vis spectrophotometry were used. Methylene blue (MB) was used as model cationic dye.[7] The Langmuir and Freundlich adsorption isotherm models were applied to describe the equilibrium isotherms. The results indicated that the data for adsorption of MB onto treated acorn shell fitted well with the Langmuir isotherm model. Comparison of adsorption capacities of CPTAS with FTAS has shown a significant increase by as much as about 30 mg/g (33.32%) in MB adsorption. The pseudo-first order, pseudo-second order kinetic models were examined to evaluate the kinetic data, and the rate constants were calculated. The rate of adsorption

was found to conform to pseudo-first-order kinetics with a good correlation. Thermodynamic parameters such as free energy, enthalpy, and entropy of dye adsorption were obtained. The acorn shell could be used as a natural adsorbent for the removal of cationic dyes.[7]

The cold plasma treatment was applied for the surface modification of bentonite to improve the removal of methylene blue (MB) from aqueous solution. The conditions for adsorption, including cold plasma time, plasma gas effect, and pH were investigated with respect to the adsorption capacity of MB. The changes of the surface property before and after cold plasma treatment were discussed. Cold plasma treated bentonite is characterized by Scanning Electron Microscopy (SEM), Fourier Transform Infrared (FTIR), BET surface area, and X-ray diffraction (XRD). Equilibrium adsorption data were analyzed by Freundlich and Langmuir equations. Langmuir isotherm exhibited the best fit with the experimental data. Adsorption kinetics were fitted with pseudo-first-order, and pseudo-second order. Cold plasma treated bentonite was exhibited largest adsorption capacity (303 mg/g) at 30°C.[8]

Experimental

All chemicals and reagents were analar purity grade. Distilled water was used for washing all glassware. The main chemicals used in this study are analytical grade $CdCl_2$ were used to make all metal ions standard solutions used in the experiments. A stock solution of 0.008M was prepared by dissolving the metal chlorides in distilled water. The pH of the metal solution was adjusted to that required by the experiment using dilute solution of hydrochloric acid and sodium hydroxide.

The concentration of metal ions was determined using two apparatus microwave plasma Atomic emission spectroscopy (4100 MP-AES, France) and Atomic Absorption Spectroscopy (AAS Vario® 6, Analytic Jena, Egypt) at 228.802 for Cd (II). Some of the samples were accordingly diluted with distilled water in order to be within the range of the assay. All glassware used for this experiment was initially cleaned to leach out any trace metals that might be present.

Adsorption of Heavy Metals

Adsorption is fixation of substances dissolved in water on solid surfaces. The effect is that the dissolved concentration is reduced. Fixation may occur by two main processes.[9]

Physical adsorption, forces of attraction between the molecules of the adsorbate and the adsorbent are of the weak van der Waals' type. Since the forces of attraction are weak, the process of physical adsorption can be easily reversed by heating or decreasing the pressure of the adsorbate.

Chemical adsorption, forces of attraction between the adsorbate and the adsorbent are very strong; the

molecules of adsorbate form chemical bonds with the molecules of the adsorbent present in the surface. The adsorption onto the zeolites proceeded by ion exchange or chemisorption mechanism.

Plasma Treatment
Zeolite-A was prepared by microwave irradiation process from Egyptian kaolin.[10] After preparation, the samples were subjected to a discharge chamber which was made from stainless steel with the dimensions of 30 x 15 x 10 cm (4.5 dm^3). A flat rectangular electrode in the upper part of the chamber was powered by the radio-frequency (rf) generator via a matching network. The rf generator operated at the industrial frequency of 13.56 MHz as shown in Fig. (1).[11]
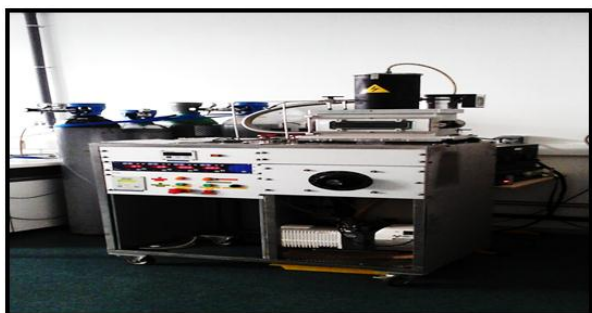
Fig. 1: Plasma Reactor.

Different parameters such as oxygen gas (O$_2$), plasma power (10, 20, 30 and 40 watt), Oxygen gas flow rate (5, 10, 20 and 30 sccm) and exposure **PLASMA** time (30 sec., 1, 3 and 6 min) was applied to determine the optimum condition to improving the surface of zeolite-A and increase the adsorption capacity for removal of cadmium ions at pH = 7.5.

Characterization Techniques
a. Microwave Plasma Atomic Emission Spectroscopy (MP-AES) and Atomic Absorption Spectroscopy (AAS)
Metal ions concentrations in solution were determined by using two apparatus microwave plasma Atomic emission spectroscopy Fig.(2) (4100 MP-AES, France) and Atomic Absorption Spectroscopy (AAS Vario® 6, Analytic Jena, Egypt) at 228.802, 340.215, 352.454 nm for Cd(II), Co(II) and Ni(II) respectively. Where metal ions present in solution were ionized until a corresponding concentration was recorded on the screen. The wavelengths and slit widths were varied to suit the optimum working range required for the particular metal ion. Before every run, the equipment was calibrated using known high grade standard solutions until a curve was obtained, which was in agreement with the calibration curves in the AAS working manual.

Fig. 2: Microwave plasma- Atomic Emission Spectroscopy.

b. Scanning Electron Micro-spectrometer (SEM) and Chemical Analysis (EDS)
The surface morphology of zeolite-A samples was determined using the Scanning Electron Micro-scopy (SEM) model (SEM, Jeol JSM- 6510 LV, France) at varying magni-fications. zeolite-A samples were coated with gold by (JEOL – JFC 1200 FINE COATER) to make their surfaces conductive and high resolution (Metallization process) as shown in Figs.(3 and 4).

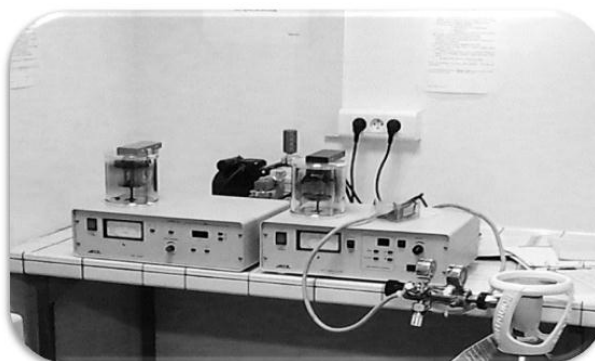**Fig. 3: Scanning Electron Microscope (JEOL - JSM 6510LV).**

Fig. 4: Metallization instrument (JEOL – JFC 1200 FINE COATER).

RESULTS AND DISCUSSION

Study the Adsorption Process of Cadmium Cd (Ii) Ions onto Zeolite-A Treated By Cold Plasma
Many studies have been reported in improving the surface properties of different materials by using cold plasma. This part is one of the first study on the modification of zeolite-A using cold plasma.

This part consists of the cold plasma treatment for modification of zeolite-A surface to improve the removal efficiency of cadmium ions from aqueous solution at pH=7.5.

To achieve this aim, the conditions for activation including cold plasma application power ranging from 10- 40 watt, plasma time between 30 sec to 360 sec. and oxygen gas flow rate from 5 to 30 sccm were investigated with respect to the adsorption capacity of cadmium ions.

The changes of the surface physical and chemical properties of prepared zeolite-A before and after cold plasma treatment were characterized by Fourier Transform Infrared with Attenuated Total Ref-lection mode (FTIR-ATR), Scanning Electron Microscopy (SEM), and X-ray diffraction (XRD). The conce-ntration of cadmium ions in aqueous was analyzed by Microwave plasma Atomic Emission Spectroscopy (MP-AES).

Study the Effect of Plasma Power
The plasma reactor was set at different plasma power from 10 to 40 watt for one minute and flow rate of oxygen gas = 10 sccm were applied to activation of zeolite-A.

Figures (5 and 6) shows the effect of cold plasma application power from 10 to 40 watt on the adsorption capacity of cadmium ions. The removal efficiency and the amount of cadmium ions adsorbed onto zeolite-A surface treated by oxygen plasma increases rapidly from 229.2 to 247.05 mg/g so amount adsorbed dependent on the power of plasma treatment and then the uptake grad-ually slow till reaching equili-brium state after about 80 min Figs. (5 and 6).
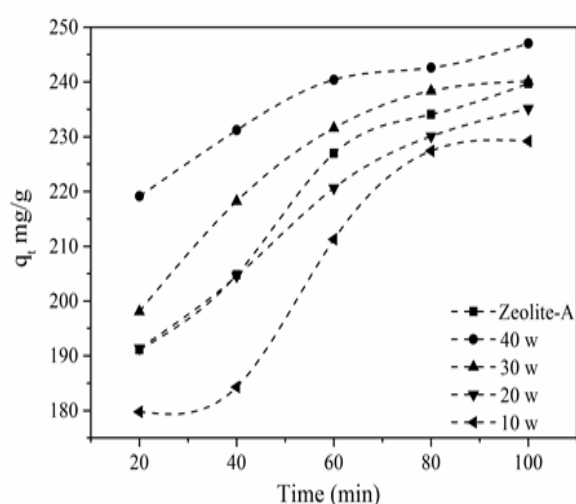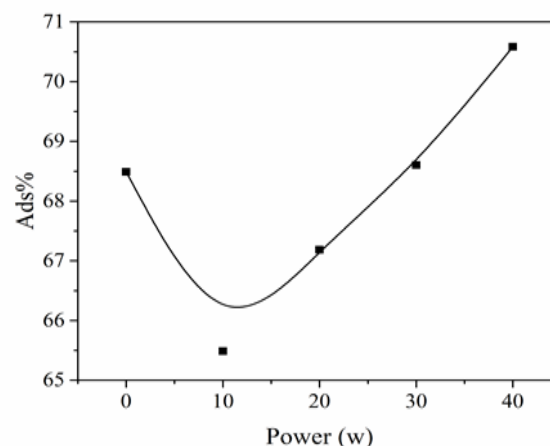
Fig. 6: Adsorption percent dependence on the different plasma power using for activation of Zeolite-A.

These results can explained in three observations: Firstly, at low energy (<10 watt) the amount of Cd ions removed were constant for ca. twenty minutes from 20 to 40 min. In generally, at low power upon 20 watt, the efficiency of adsorption was lower than that recorded for blank one zeolite-A (UZA$_{Cd}$). This behavior may be due to particles of zeolite-A charged by thousands of electrons and/ or radicals during plasma treatment. These trapped of electrons or radicals form plasma sheath around the particle at the same time, and strong Coulomb repulsions exist between the electrons and radicals trapped on the same particle so the sorption capacity of blank zeolite-A (UZA) was higher than treated at power upon 20 watt as shown in (Fig. 5).[12] Secondly, at high power upon 40 watt the adsorption rate of modified zeolite-A (TZA$_{Cd}$) by plasma O$_2$ was increased from 229 to 247 mg/g (removal of cadmium $\approx$ 72%) Figs. (5 and 6).

The reason, if the energy was sufficient, the active species such as high-energy electrons and reactive radicals were generated during plasma and can activate the surface of zeolite-A by increasing the number of active sites or/and creates functional groups like oxygen groups. On the other side, if it was not enough, this energy may be acting as only a cleaner for the surface of zeolite. However, excessive plasma treatment led to destruction of surface functional groups of zeolite-A.[13] Moreover, it was expected that ion-exchange will be the main adsorption mechanism of cadmium ions onto zeolite-A, where mainly Na$^+$ ions will be replaced by cadmium ions [14]. Thirdly, the equilibrium of adsorption occur at 80 min, approximately when all active centers on the surface of zeolite-A were blocked by Cd(II) ions from solution.[15]

Fig. 5: Relationship between contact time and adsorption capacity at various plasma power, plasma time and flow rate of oxygen gas = 60 sec. and 10 sccm, respectively.

Ir-Atr Analysis of Zeolite-A, Zeolite-A Treated By Oxygen Plasma at Different Power and After Adsorption of Cadmium Ions
IR-ATR analysis was carried out to identify the main functional groups of zeolite-A before and after plasma

treatment which were responsible for the adsorption of cadmium ions Fig. (7) The spectra of the samples were measured in the wave number range of 400–4000 cm^{-1}.
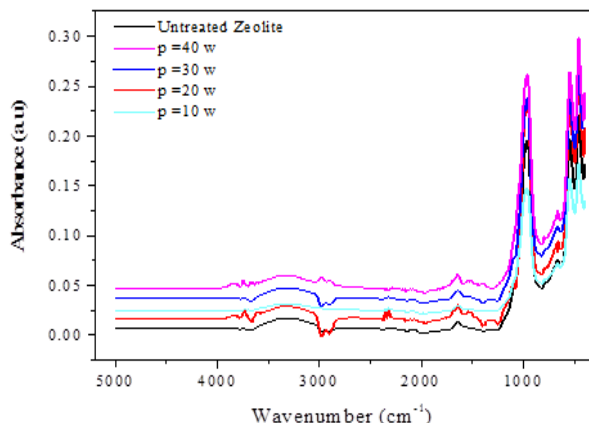

Fig. 7: IR.ATR spectra for Zeolite-A after treatment by plasma at different power (10-40 watt), plasma time and flow rate of oxygen gas = 60 sec. and 10 sccm, respectively.
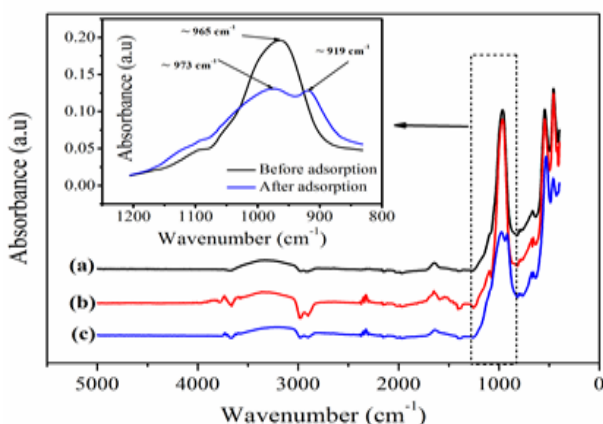

Fig. 8: IR-ATR spectra of (a, b) untreated Zeolite-A (blank) and Zeolite-A treated by plasma at power=40 watt, respectively (c) Zeolite-A after adsorption of Cd (II) ions.

The characteristic peaks of zeolite-A at 998 cm^{-1}, 970 cm^{-1} and 671 cm^{-1} were represented to the (Si-O). Peak at 555 cm^{-1} was belong to O-Si-O bonds in the SiO_2 molecules. The peak at 461 cm^{-1} was assigned to Si-O-Si for more details see.[16]

The IR-ATR spectrum of the studied zeolite-A before the adsorption process Fig. (7) displays a number of absorption peaks, a broad peak at 3298 cm^{-1} which was represented to the O–H stretching.[17,18] While change during plasma treatment is the increase of the broad band at 3660–3070 cm^{-1} that was related to desorption and/or condensation of adsorbed (HO)Si≡ species.[19] Peak at 965 cm^{-1} was assigned to Si-O bonds vibration in the SiO_4 molecules. Absorption band that was observed at ~534 cm^{-1} may be associated to Si-O-Al stretching vibration where the Al is in octahedral coordination.[20]

The peaks in the range of 1000-900 cm^{-1} indicates the presence of Si-O and the crystallization peaks appear in the zone of absorption 555 - 501 cm^{-1} which is referred to the presence of structural double rings of zeolites.[21] After treatment of zeolite-A by the cold plasma O_2 the characteristic peaks became sharper and more intense, compared to zeolite-A before modification especially at plasma power=40 watt. Probably, this observation is due to the changes at the surfaces of the zeolite-A particles as seen in Fig. (7).

Figure (8) shows the IR-ATR of zeolite-A after the adsorption of cadmium ions. The broad peak at 3298 cm^{-1} is decreased in broadening due to adsorption of cadmium and formation of hydrogen bond. The peak at wavenumber ~ 965 cm^{-1} becomes less intense than before adsorption of cadmium ions and separated into two peaks indicating that a new peak which related to cadmium ions appeared at ~ 919 cm^{-1} for (Si—O—Cd). These may be as a result of the bond formed between cadmium ions and active centers on the surface of zeolite-A, and the second peak for Si—O at 973 cm.[1,22]

Sem-Eds Analysis Of Zeolite-A And Zeolite-A Treated By Plasma Before And After Adsorption Of Cadmium Cd(Ii) Ions
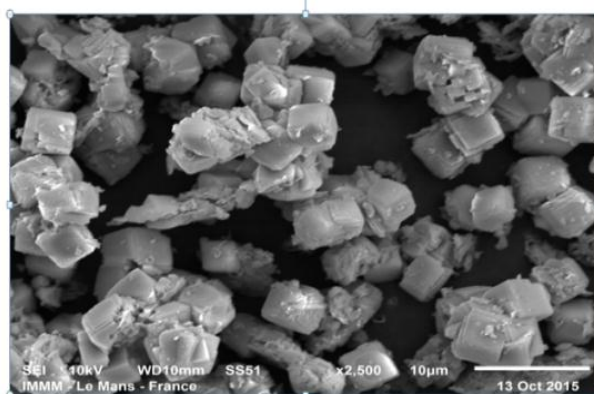
Fig. (13) SEM image for Zeolite-A treated by plasma at p=40 watt,   t= 60 sec. and flow rate= 10 sccm
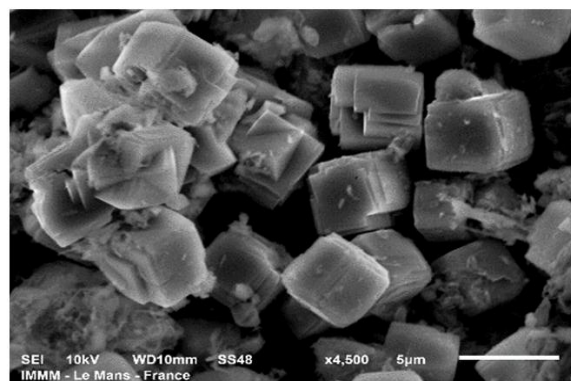

Fig. (9) SEM image for untreated Zeolite-A

In the SEM analysis, Figs. (9-13) are showing the change in zeolite-A surfaces before and after plasma treatment at

different power from 10 to 40 watt. It is clear that, well-developed uniform cubic crystallites typical morphology of zeolite-A are well defined with an average grain size of less than 5 μ Fig. (9). It is worth mentioning that, plasma treatment has no phase effect on the cubic structure surfaces Fig. (10-13) which confirms the XRD results.[23,24]
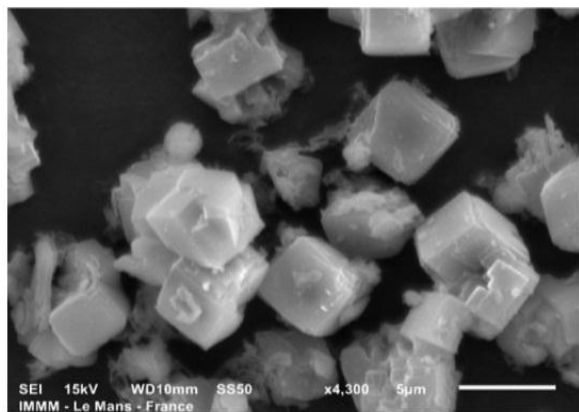

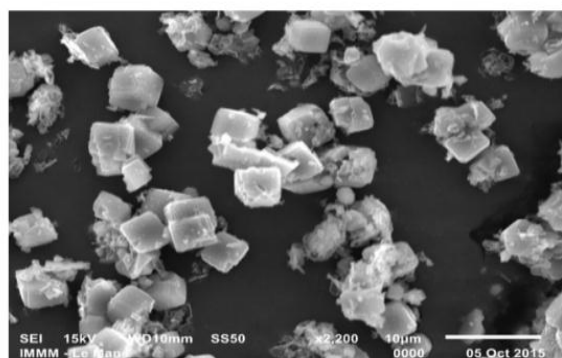Fig. (11) SEM image for Zeolite-A treated by plasma at p=20 watt, t= 60 sec. and flow rate= 10 sccm

Fig. (10) SEM image for Zeolite-A treated by plasma at p= 10 watt, t= 60 sec. and flow rate= 10 sccm
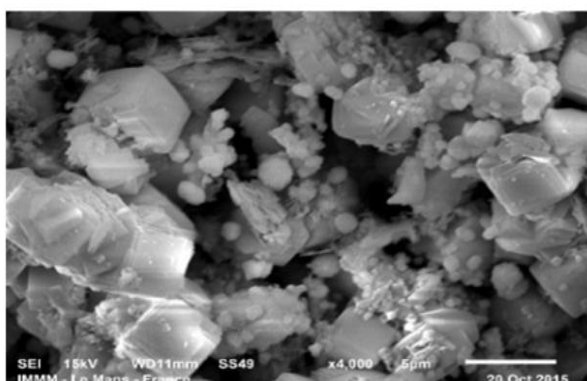
Fig. (14) SEM image of untreated Zeolite-A after adsorption of cadmium ions
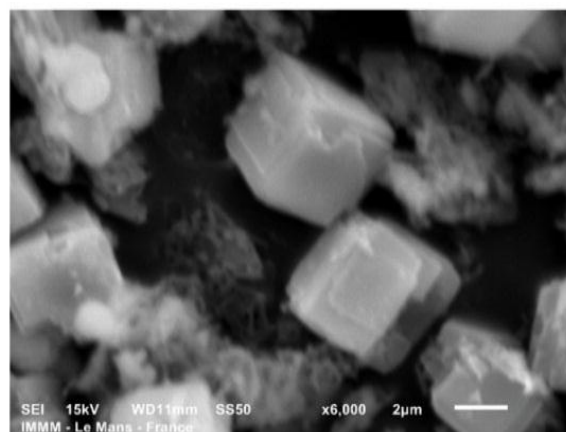
Fig. (12) SEM image for Zeolite-A treated by plasma at p=30 watt, t= 60 sec. and flow rate= 10 sccm

Figures (14-18) depicts the effect of cadmium exchange process on untreated zeolite-A surface before and after treatment by plasma, where the crystals are slightly reduced in size (4-4.5 μ) with some undifferentiated structures with rounded edges. This behavior probably due to cadmium ions were adsorbed onto the surface of zeolite-A particles. After adsorption of cadmium ions, the crystals were showed more bright color and more rounded morphology due to cadmium exchange. The bright color may be due to the interaction between the electron beam and the cadmium ions inside the crystals whereas the rounded surfaces can be explained by the adsorption of cadmium onto the newly developed active sites on zeolite surface by plasma effect. The adsorption mechanism by ion exchange inside pores (inner) and surface adsorption (outer) are reported as the possible two mechanisms for adsorption of cadmium ions onto zeolite-A.[14,25]
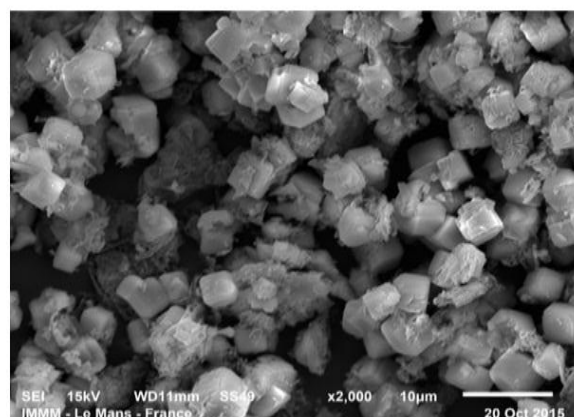
Fig. (15) SEM image of Zeolite-A treated by plasma at power=10 watt after adsorption of cadmium ions, plasma time and flow rate of oxygen gas = 60 sec. and 10 sccm, respectively
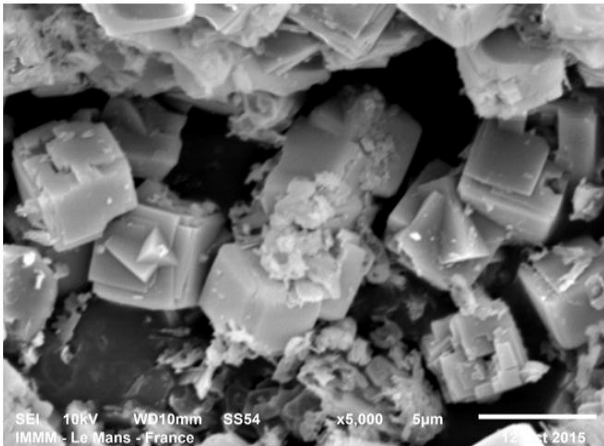
Fig. (17) SEM image of Zeolite-A treated by plasma at power=30 watt after adsorption of Cd(II) ions, plasma time and flow rate of oxygen gas = 60 sec. and 10 sccm, respectively
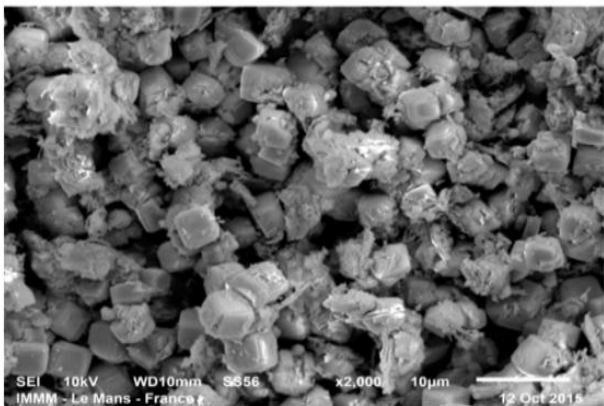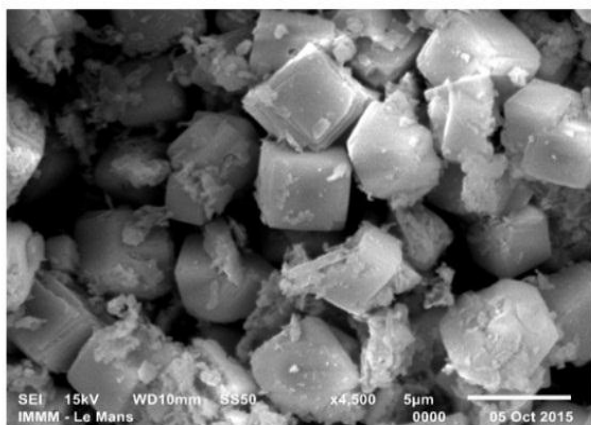

Fig. (16) SEM image of Zeolite-A treated by plasma at power=20 watt after adsorption of cadmium ions, plasma time and flow rate of oxygen gas = 60 sec. and 10 sccm, respectively

Fig. (18) SEM image of Zeolite-A treated by plasma at power=40 watt after adsorption of Cd(II) ions, plasma time and flow rate of oxygen gas = 60 sec. and 10 sccm, respectively

Figure (19) implies the chemical micro analysis of the parent (UZA), plasma treated (TZA) at plasma power 40 watt, time= 60 sec. and flow rate of oxygen gas = 10 sccm, untreated cadmium (UZA$_{Cd}$) and treated cadmium zeolite-A (TZA$_{cd}$) respectively which reveals the Si/Al ratio is about near to unity which is the known ratio for zeolite-A composition given by the XRD formula

$Na_{12}Al_{12}Si_{12}O_{48}.27H_2O$, (all samples metalized with gold by using fine coater).[26]
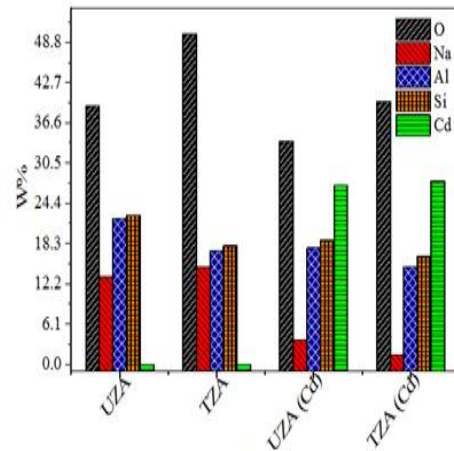
Fig. (19) Chemical microanalysis of untreated Zeolite-A, treated at plasma power =40 watt and after adsorption of Cd(II) ions
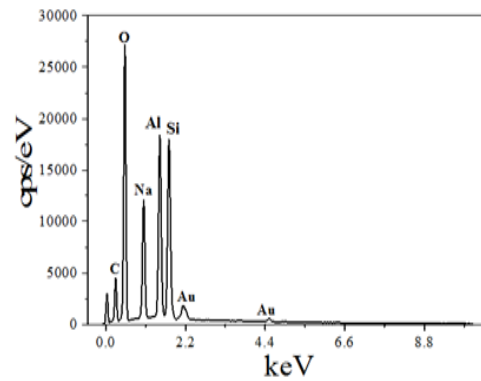
Fig. (20) The micrographs of the elemental analysis of TZA at plasma power 40 watt, plasma time = 60 sec. and flow rate of oxygen gas= 10 sccm, respectively
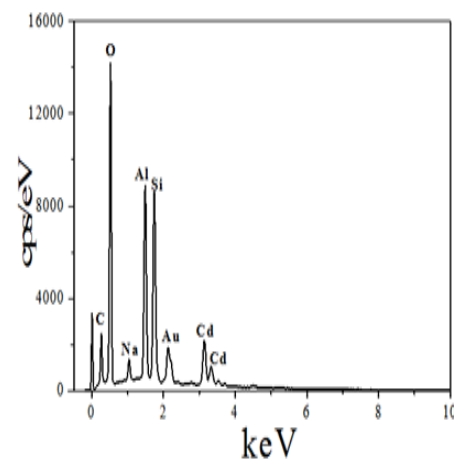
Fig. (21) The micrographs of the elemental analysis of TZA$_{Cd}$ (after adsorption od cadmium ions, at plasma power =40 watt, plasma time = 60 sec. and flow rate of oxygen gas= 10 sccm, respectively
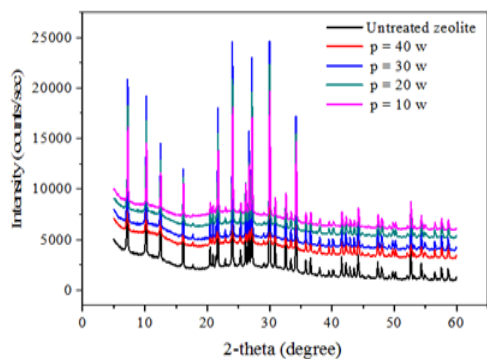
Fig. (22) X-ray diffraction patterns of the parent (UZA), plasma treated Zeolite-A at different power from 10 to 40 watt
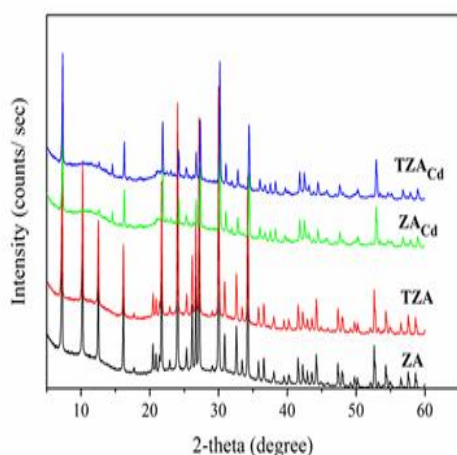

Fig. (23) X-ray diffraction patterns of the parent (UZA), plasma treated (p=40 watt) (TZA), untreated cadmium (UZA_Cd) and treated cadmium Zeolite-A (TZA_Cd) respectively

Figure (19) show an increase in the weight percentage of oxygen content (50.05 %) of the plasma treated sample (TZA) than that of untreated zeolite (UZA), which could be related to the effect of plasma in creating centers of new active group on zeolite structure [27,28]. The data of the 100% sodium content per zeolite formula is (13.2 %) for UZA, this percent is reduced to 3.63 % and 1.37 % in UZA_Cd, TZA_Cd, respectively Whereas, the corresponding wt% of Cd^{+2} is increased from 0.0 to 27.16 and 27.77 in the same direction, indicating the retention of cadmium at the expenses of sodium onto zeolite framework. Although, the amount of exchanged sodium by cadmium for TZA_Cd (90.7%) is higher than that of UZA_Cd (72.5%), the cadmium Wt. % is nearly the same (27.77 & 27.16). It is also noticed that the amount of Al and Si (main skeleton of zeolite) are also reduced in TZA_Cd which could be due to the instability of zeolite structure under cadmium exchange process as previously mentioned in XRD results. Similar results was reported in.[29,30] which confirms the XRD data. It is known that Al is readily dissolved than Si that is the reason of much reduction in Al than that of Si, since the Al content of particular zeolite is related to it is cation exchange capacity (CEC). Probably, the mechanism of cadmium removal in this case is done by CEC and surface adsorption on the active sites. Figures (20,21) represent the micrographs of the elemental analysis of TZA and TZA_Cd.

X-Ray Diffraction Of The Parent (Uza), Plasma Treated (Tza), Untreated Cadmium (Uza_cd) And Treated Cadmium Zeolite-A (Tza_cd)

Figure (22) shows the XRD patterns of the blank Zeolit-A (UZA), plasma treated (TZA) at different power from 10 to 40 watt. The sharp and strong peaks of the XRD pattern indicated a well crystalline material with complete match with Linde Type A (LTA) PDF #73-2341 with $Na_{12}Al_{12}Si_{12}O_{48}.27H_2O$. It is clear that treating zeolite with plasma is not affecting the peak intensities and positions, indicating that the plasma treatment had no effect on the basic structure of zeolite samples [23,24].

Figure (23) reveals the pattern for untreated zeolite-A, treated by plasma at power=40 watt, after adsorption of cadmium ions UZA_Cd and treated cadmium zeolite-A (TZA_cd) respectively. Notably, the peaks of cadmium – loaded zeolite (treated and untreated) showed some peak reduction which may be explained by the instability of zeolite powder in the relative acidic media for two hours (approx.) of cadmium treatment compared to the strongly basic one of it is synthesis [29,30]

Effects of Different Flow Rate of Oxygen Gas and Plasma Time

A plasma reactor with continuous output power was applied for treatment of prepared adsorbent. zeolite-A was placed in a chamber of reactor and allow to introduction of oxygen gas flow at different rate (5-30 sccm), plasma power=40 watt and time= 60 sec. The third condition to activation of zeolite-A is exposure plasma time, in this case the reactor was set at different plasma time (30-360 sec.), plasma power=40 watt and flow rate of oxygen gas =10 sccm were applied to treatment of zeolite-A and study the modification effects.

The curves of adsorption of cadmium ions on the untreated and treated zeolite-A (UZA and TZA) surfaces as a function of flow rate of oxygen gas (from 0 to 30 sccm) and the plasma time (from 30 to 360 sec.) are shown in Figs. (24, 26).

Figures (25, 27) reveals the removal efficiency of cadmium ions from aqueous phase at different flow rate of oxygen gas was increased from 68.5% to 79.3%, while the plasma application time was prolonged from 0 sec (untreated plasma) to 360 sec. by increasing plasma time from 0 to 1 min the removal percentage of cadmium ions increased from 68.5% to 70.6%, but after 1 min, the percentage of removed cadmium ions was decreased to 59.6% and the adsorption capacity of cadmium was 208.6 mg/g.
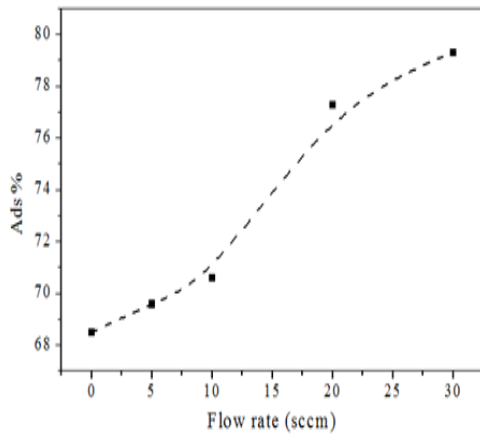
Fig. (25) Adsorption percentage dependence on the different flow rate of oxygen gas using for activation of Zeolite-A
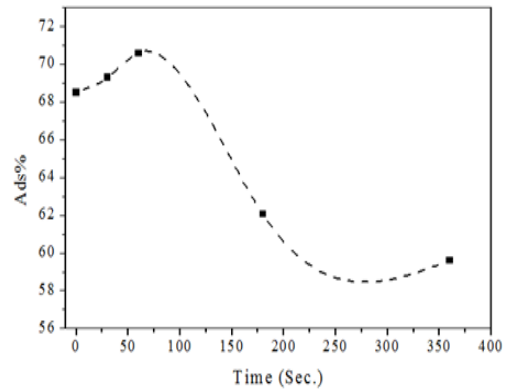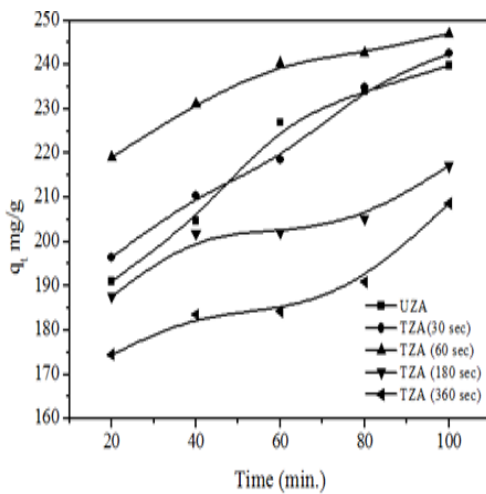

Fig. (26) Relationship between contact time and adsorption capacity of Cd(II) ions at various plasma time, plasma power and flow rate of oxygen gas = 40 watt and 10 sccm, respectively
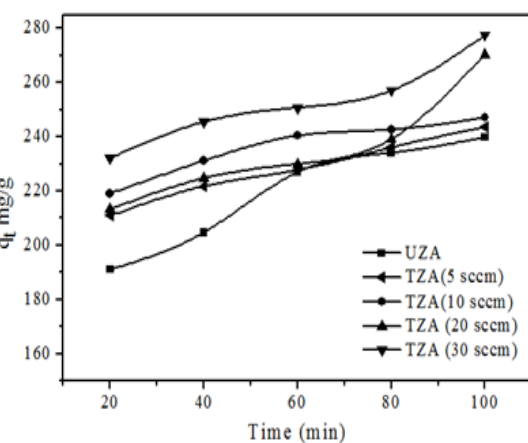

Fig. (24) Relationship between contact time and adsorption capacity of Cd(II) at various flow rate of oxygen gas, plasma power and time = 40 watt and 60 sec., respectively

Fig. (27) Adsorption percentage dependence on the different plasma time using for activation of Zeolite-A

It was observed in Fig. (25) that increasing the flow rate of oxygen gas (5, 10, 20 and 30 sccm) leads to increase the removal efficiency by 68.5%, 69.6%, 70.6%, 77.3% and 79.3% , respectively. This increasing is due to creation of new functional groups on the surface of adsorbent like (oxygen groups) [27].

On the other hand, the amount of cadmium ions adsorbed on the surface of zeolite-A with and without plasma time (UZA,TZA) treatment increased rapidly from 0 to 60 sec. and then decreases till reaching about 360 sec. notably, excessive cold plasma time treatment depressed the specific surface composition of prepared zeolite-A. It is worth mentioning that this phenomenon takes place due to the destruction of active centers on the surface of zeolite-A as seen in Fig. (27) [31]

Ft-Ir Analysis For Zeolite-A Treated By Plasma (At Different Plasma Time And Flow Rate Of Oxygen Gas) And Treated With Cadmium Cd (Ii) Ions
Figures (28-31) illustrates the FT-IR absorbance spectra of untreated zeolite-A (UZA), treated zeolite-A by plasma (TZA) at different flow rate (5-30 sccm) and exposure plasma time (30-360 sec.) and treated with cadmium ions (UZA$_{Cd}$ and TZA$_{Cd}$) in ATR mode.
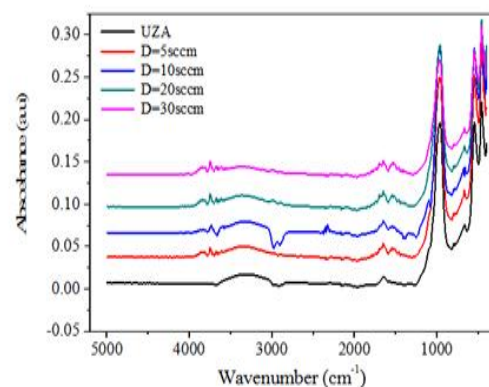

Fig. (28) IR-ATR Spectra of the untreated Zeolite-A (UZA) and Zeolite-A treated by plasma (TZA) at different flow rate of oxygen gas, plasma power and time = 40 watt and 60 sec., respectively
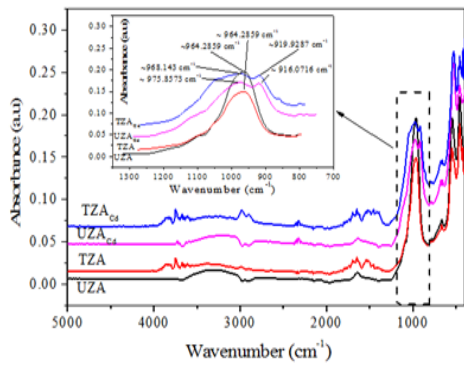
Fig. (29) IR-ATR Spectra of the untreated Zeolite-A (UZA), plasma treated (TZA) at flow rate = 10 sccm, untreated cadmium (UZA_Cd) and treated cadmium Zeolite-A (TZA_Cd)
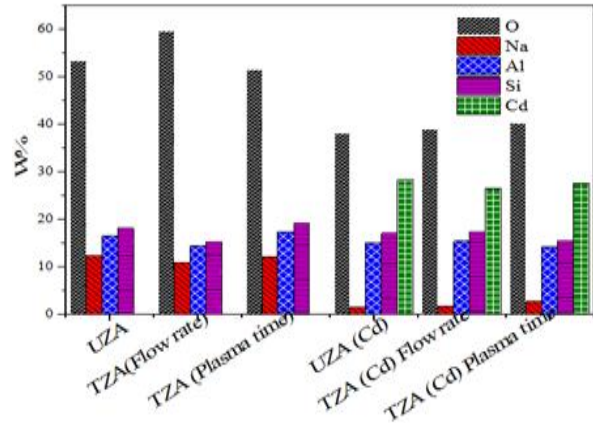

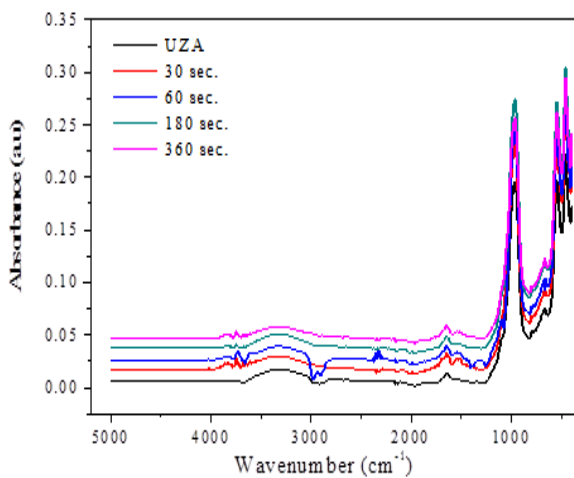Fig. (50) Chemical microanalysis of untreated and treated Zeolite-A powders

Fig. (31) IR-ATR Spectra of the untreated Zeolite-A (UZA), plasma treated (TZA) at plasma time = 60 sec., untreated cadmium (UZA_Cd) and treated cadmium Zeolite-A (TZA_Cd).
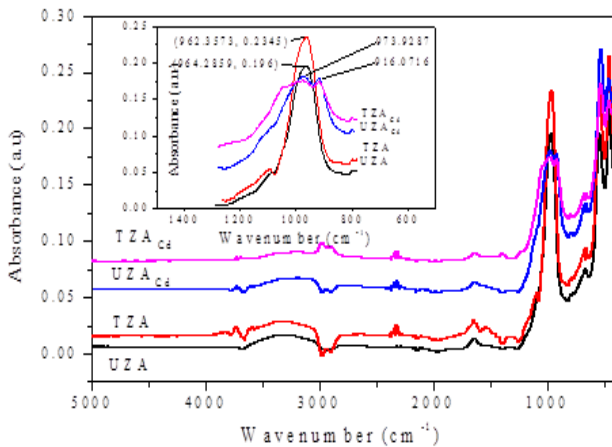
In general, the spectrum revealed that the parent zeolite- and treated zeolite-A had essentially the same characteristic species of functional groups on the surface. The IR-ATR spectra of the raw (UZA) and cold plasma - treated samples (TZA) have the typical bands at ~3310 cm^{-1} (-OH stretching); ~960 cm^{-1} (Si-O stretch) and 900–950 cm^{-1} (Al-OH vibration). During plasma treatment (plasma time) an important changes were observed in the cold plasma treated zeolite-A. An overall increase in the broading of the -OH stretching bands was observed, which attributed to -OH stretching of silanol group (Si-OH) with adsorbed water Absorption band that was observed at ~540 cm^{-1} may be associated to Si-O-Al stretching vibration where the Al is in octahedral coordination and the crystallization peaks appear in the zone of absorption ~ 555 - 501 cm^{-1} which is referred to the presence of (Si–O–Si) structural double rings of zeolites [16,20,21]. After treatment of zeolite-A by the plasma especially at different time the characteristic peaks became sharper and more intense, compared to zeolite-A before activation. Probably, this observation is due to the functional groups changes at the surfaces of the zeolite-A particles shown in Figs. (28,30)

Figures (29,31) shows the IR analysis of zeolite-A after the adsorption of cadmium ions (UZA_Cd) and (TZA_Cd). The broad peak at ~ 3310 cm^{-1} is decreased in broadening due to adsorption of cadmium and formation of hydrogen bond. The peak at wavenumber ~ 960 cm^{-1} and 962 cm^{-1} becomes less intense than before adsorption of cadmium ions and separated into two peaks indicating that a new peak which related to cadmium ions appears at ~916 cm^{-1} and ~919 cm^{-1} for Si—O—Cd as seen in figs. (29 and 31). These may be as a result of the interaction between cadmium ions and active functional groups on the surface of treated and untreated zeolite-A (UZA_Cd and TZA_Cd), the second peak for Si—O at ~973-975 cm^{-1}.[22]

Fig. 30: IR-ATR Spectra of the untreated Zeolite-A (UZA) and Zeolite-A treated at different plasma time, plasma power and flow rate of oxygen gas = 40 watt and 10 sccm, respectively.
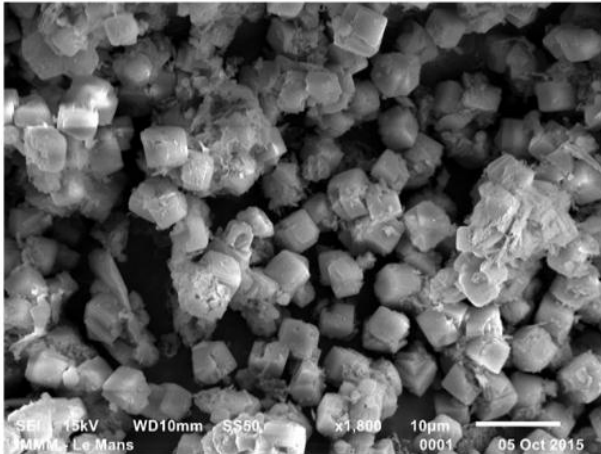
Fig. (33) SEM image of treated Zeolite-A by plasma at flow rate of oxygen gas = 5 sccm

Sem-Eds Analysis For Zeolite-A Treated By Plasma (At Different Plasma Time And Flow Rate Of Oxygen Gas) And Treated With Cadmium Cd(Ii) Ions

SEM images of the parent zeolite-A (UZA), cold plasma treated zeolite-A samples at different flow rate of oxygen gas and plasma time (TZA) and zeolite-A after adsorption of cadmium ions (UZA$_{Cd}$, TZA$_{Cd}$) are shown in Figs. (32-40). There are no differences in the morphology of the parent and cold plasma treated zeolite-A samples. As observed in SEM images, the untreated sample was formed by cubic structure closely to each other. Compared to the untreated sample, the treated one with non-thermal plasma, the particles had a more regular edge and smoother surface, which appeared to the characteristics of crystallization. This crystal appearance probably occurs due to the change in the surface charge of the particle because of cold plasma modification process Figs. (33-40).[32]

It is worth mentioning that, plasma treatment at different flow rate of O$_2$ gas and plasma time has no phase effect on the cubic structure surfaces which confirms the XRD results.[23,24]
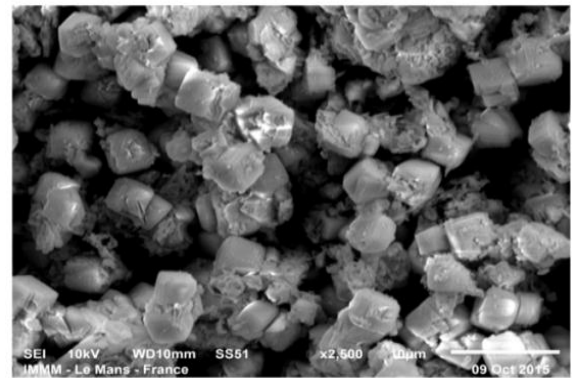
Fig. (34) SEM image of treated Zeolite-A by plasma at flow rate of oxygen gas = 10 sccm
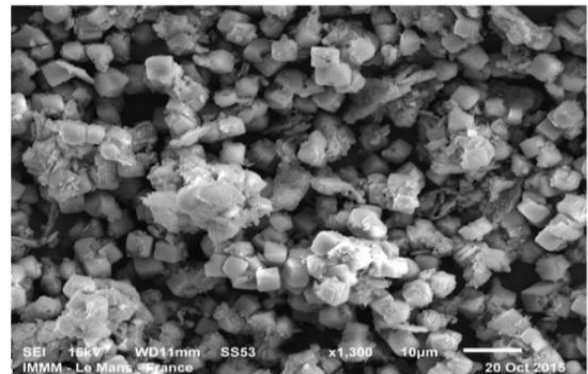

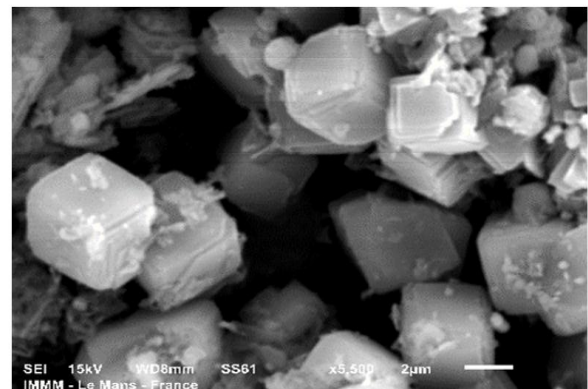Fig. (35) SEM image of treated Zeolite-A by plasma at flow rate of oxygen gas = 20 sccm

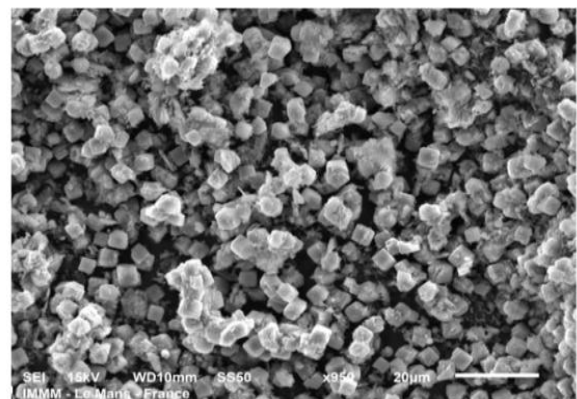Fig. (36) SEM image of treated Zeolite-A by plasma at flow rate of oxygen gas = 30 sccm

Fig. (32)SEM image of untreated Zeolite-A

Fig. (37) SEM image of treated Zeolite-A at different plasma time t=30 sec.
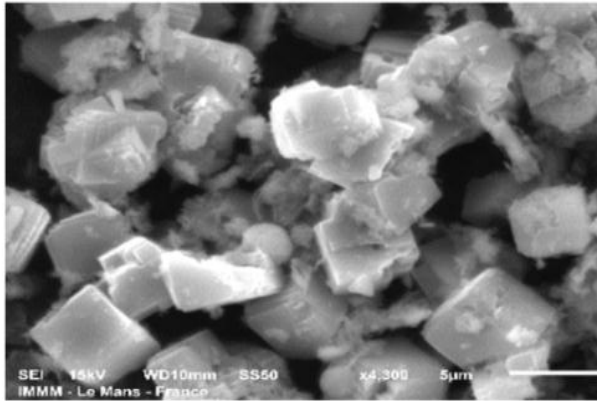
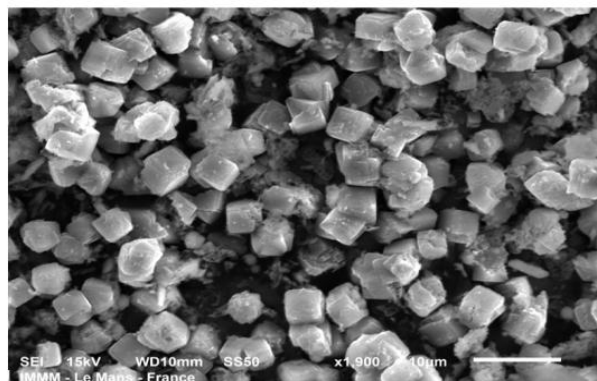Fig. (38) SEM image of treated Zeolite-A at different plasma time t=60 sec.

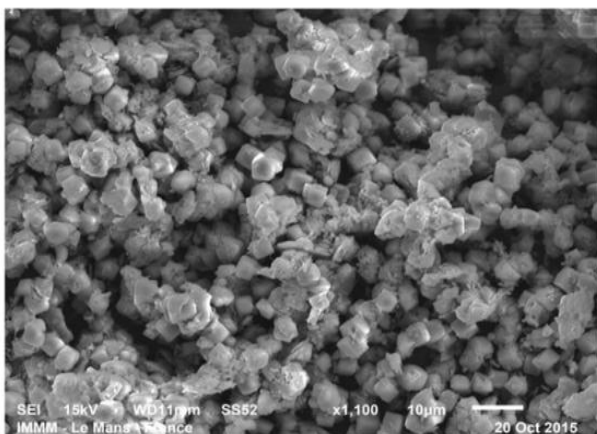Fig. (40) SEM image of treated Zeolite-A at different plasma time t=360 sec.

Fig. (39) SEM image of treated Zeolite-A at different plasma time t=180 sec.

active sites on zeolite surface by plasma effect as mentioned before. The possible two mechanisms for adsorption of cadmium ions onto the surface of zeolite-A by ion exchange inside pores and surface adsorption.[14,25]
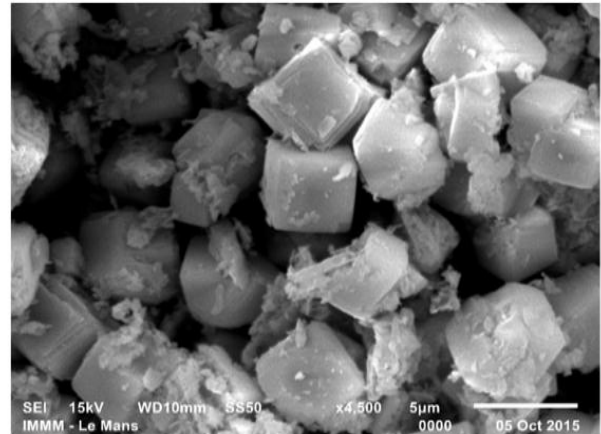

Fig. (43) SEM image of treated Zeolite-A by plasma at flow rate of oxygen gas = 10 sccm, after adsorption of Cd(II) ions
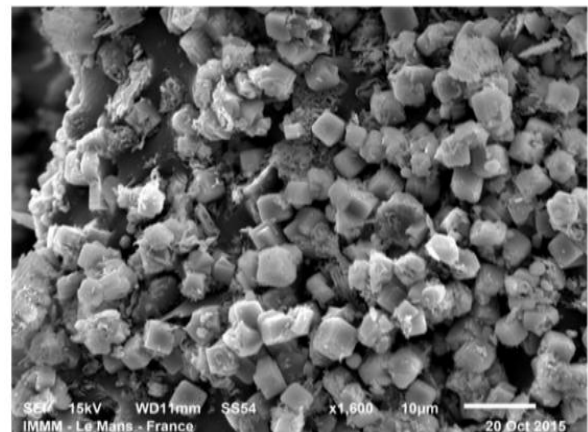

Fig. (42) SEM image of treated Zeolite-A by plasma at flow rate of oxygen gas = 5 sccm, after adsorption of Cd(II) ions
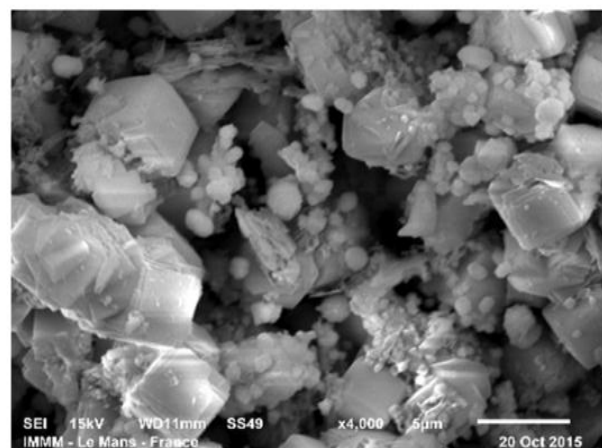

Fig. (41) SEM image of untreated zeolite-A after adsorption of Cd(II) ions

Figures (41-49) reveals the effect of cadmium exchange process on zeolite-A surface, where the crystals are slightly reduced in size with some undifferentiated structures with rounded edges. This reason is due to the presence of the crystals of the cadmium chloride solution of the exchange process. After adsorption of cadmium ions, the crystals show more bright color and more rounded morphology due to cadmium adsorbed. The bright color may be referred to the interaction between the electron beam and the adsorbate ions inside the crystals whereas the rounded surfaces can be explained by the adsorption of cadmium onto the newly developed
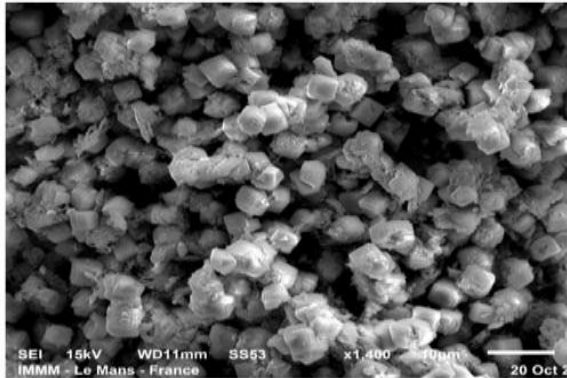
Fig. (44) SEM image of treated Zeolite-A by plasma at flow rate of oxygen gas = after adsorption of Cd(II) ions
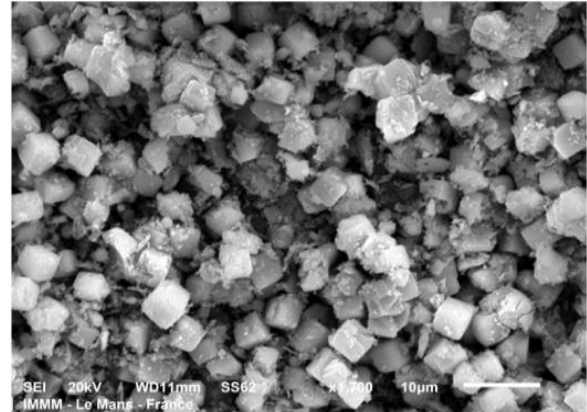

Fig. (47) SEM image of treated Zeolite-A at plasma time = 60 sec., after adsorption of Cd(II) ions
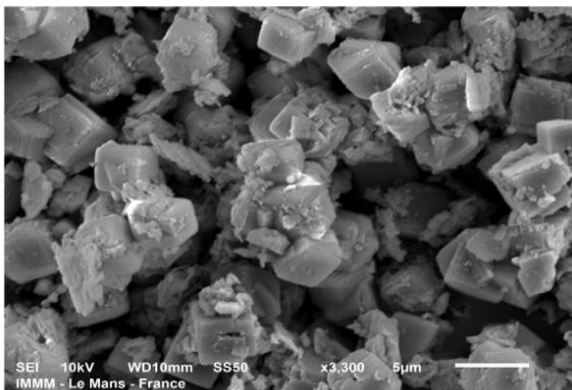

Fig. (45) SEM image of treated Zeolite-A by plasma at flow rate of oxygen gas = 30 sccm, after adsorption of Cd(II) ions
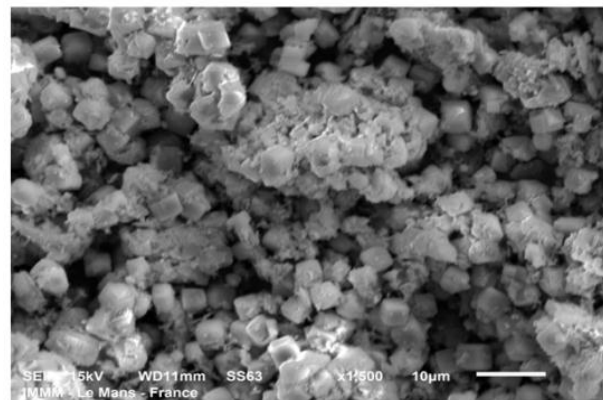

Fig. (48) SEM image of treated Zeolite-A at plasma time = 180 sec., after adsorption of Cd(II) ions
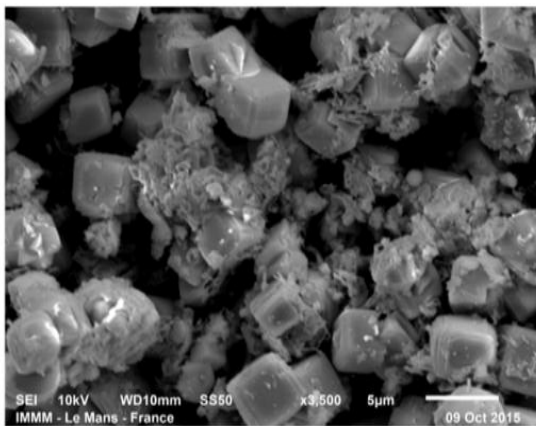

Fig. (46) SEM image of treated Zeolite-A at plasma time = 30 sec., after adsorption of Cd(II) ions
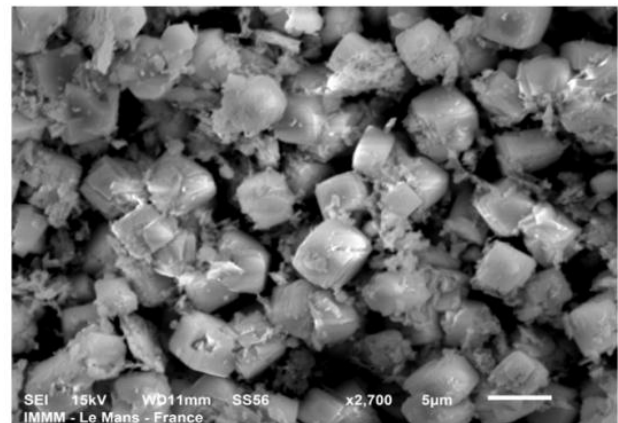

Fig. (49) SEM image of treated Zeolite-A at plasma time = 360 sec., after adsorption of Cd(II) ions

Figure (50) determines the chemical analysis of the untreated zeolite-A (UZA), plasma treated (TZA) at plasma time=60 sec. and flow rate of oxygen gas= 10 sccm, untreated cadmium UZA_{Cd} and treated cadmium zeolite-A (TZA_{cd}), respectively which indicate the Si/Al ratio is about near to unity which is the known ratio for zeolite-A composition given by the XRD formula $Na_{96}Al_{96}Si_{96}O_{384}.27H_2O$.[26]

Similar results was reported in,[29,30] which confirms the XRD data. It is known that Al is readily dissolved than Si that is the reason of much reduction in Al than that of Si, since the Al content of particular zeolite is related to it is cation exchange capacity (CEC). Probably, the mechanism of cadmium removal in this case is done by interaction with active sites on the surface of zeolite-A.

X-Ray Diffraction For Zeolite-A Treated By Plasma (At Different Plasma Time And Flow Rate Of Oxygen Gas) And Treated With Cadmium Cd(Ii) Ions
The crystallinity and purity of zeolite-A particles have been investigated by XRD. Figures (51-54) shows the powder X-ray diffraction patterns of the synthetic zeolite-A (UZA), zeolite-A treated by plasma at different flow rate of gas and plasma time (TZA) and zeolite-A treated by cadmium ion solution (UZA$_{Cd}$, TZA$_{Cd}$).

The sharp and strong peaks of the XRD pattern indicated a well crystalline material with complete match with Linde Type A (LTA) PDF #73-2341 with Na$_{12}$Al$_{12}$Si$_{12}$O$_{48}$.27H$_2$O. It is clear that treating zeolite with plasma at two conditions is not affecting the peak intensities and positions, indicating that the plasma treatment had no effect on the basic structure of zeolite samples Figs. (51, 52) as discussed before.[14,23]
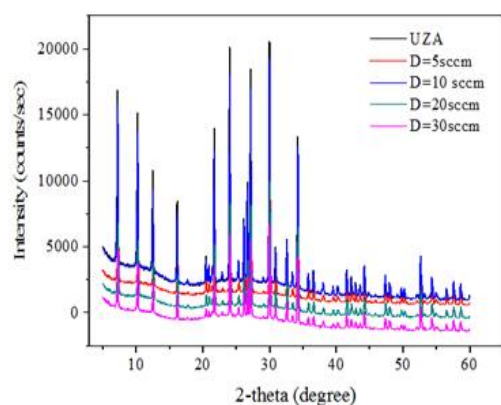

Fig. (51) X-ray diffraction patterns of the untreated Zeolite-A (UZA), plasma treated (TZA) at different flow rate of oxygen gas, plasma power and time = 40 watt and 60 sec., respectively
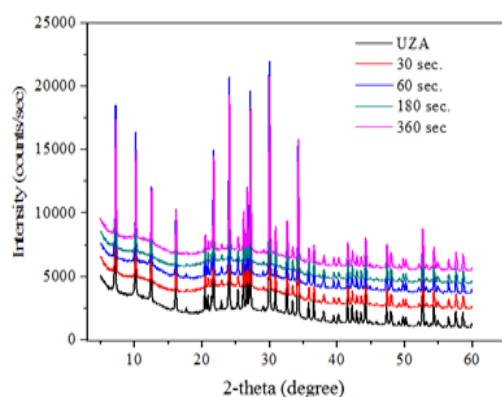

Fig. (52) X-ray diffraction patterns of the untreated Zeolite-A (UZA), plasma treated (TZA) at plasma time, plasma power and flow rate of oxygen gas = 40 watt and 10 sccm, respectively

The XRD patterns consist of mainly peaks characteristic of zeolite-A. Notably, the peaks of cadmium – loaded zeolite (treated and untreated) showed peak reduction at 2θ, (12.5°) which may be explained by the instability of zeolite crystals in the relative very weak basic media for two hours (approx.) of cadmium treatment compared to the strongly basic one of it is synthesis as represented in Figs. (53,54).[24,30]
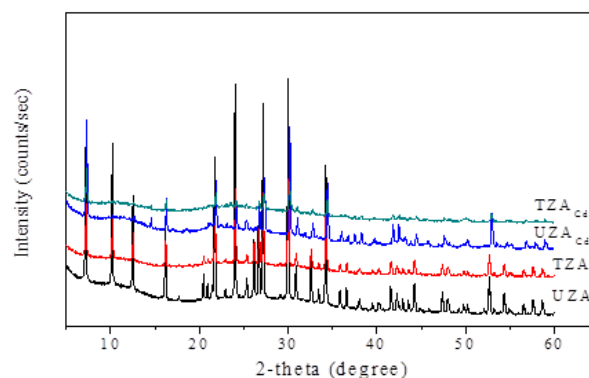

Fig. 53: X-ray diffraction patterns of the untreated Zeolite-A (UZA), plasma treated (TZA) at flow rate= 10 sccm, untreated cadmium (UZA$_{Cd}$) and treated cadmium Zeolite-A (TZA$_{Cd}$), respectively.
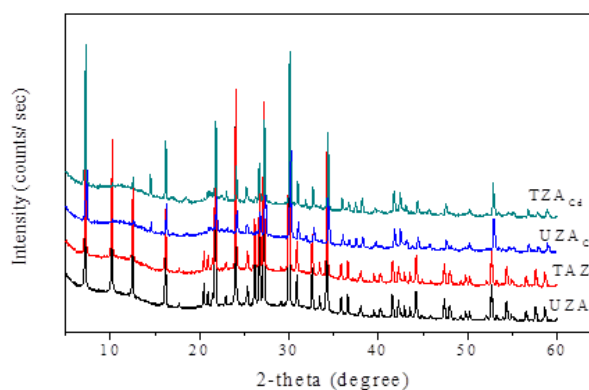

Fig. 54: X-ray diffraction patterns of the untreated Zeolite-A (UZA), plasma treated (TZA) at plasma time = 60 sec., untreated cadmium (UZA$_{Cd}$) and treated cadmium.

REFERENCES

1. N. Koshy, D. N. Singh; Journal of Environmental Chemical Engineering, 2016; 4: 1460–1472.
2. E. B. G. Johnson, S. E. Arshad; Applied Clay Science, 2014; 97–98; 215–221.
3. L. Ayele, J. Perez-Pariente, Y. Chebude, I. Díaz; Microporous and Mesoporous Materials, 2015; 215: 29-36.
4. H. S. Ibrahim, T. S. Jamil, E. Z. Hegazy; Journal of Hazardous Materials, 2010; 182: 842–847.
5. Q. Cai, B. D. Turner, D. Sheng, S. Sloan; Journal of Conta-minant Hydrology, 2015; 177–178-136–147.
6. F. Poncin-Epaillard, T. Vrlinic, D. Debarnot, M. Mozetic, A. Coudreuse, G. Legeay, B. El Moualij,

W. Zorzi; Journal of Functional Biomaterials, 2012; 3: 528-543.

7. C. Saka, O. Sahin, H. Adsoy, S. M. Akyel; Separation Science and Technology, 2012; 47: 1542–1551.

8. O. Şahin, M. Kaya, C. Saka; Applied Clay Science, 2015; 116–117: 46–53.

9. Ch. Baerlocher, W. M. Meier, D.H. Olson, Atlas of Zeolite Framework Types (Eds.) 5th edition, Elsevier, Amsterdam, 2001.

10. H. Youssef, D. Ibrahim, S. Komarneni; Microporous and Mesoporous Materials, 2008; 115: 527–534.

11. T. Vrlinic, C. Miller, D. Debarnot, F. Poncin-Epaillard; Vacuum, 2009; 83: 792–796.

12. H. Javadian, F. Ghorbani, H. Tayebi, S.H. Asl; Arabian Journal of Chemistry, 2013; 8: 837–849.

13. Fahmy, A. Schönhals, J. Friedrich; Journal of Physical Chemistry B, 2013; 117: 10603-10611.

14. L. Remenarova, M. Pipıska, E. Florkova, M. Hornık, M. Rozloznık, J. Augustın; Clean Technology and Env-ironmental Policy, 2014; 16: 1551-1564.

15. O. Moradi; Chemical and Biochemical Engineering Quarterly, 2011; 25(2): 229–240.

16. H. F. Youssef, W. H. Hegazy, H. H. Abo-almaged; Journal of Porous Mate-rials, 2015; 22: 1033-1041.

17. N. Feng, X. Guo, S. Liang; Journal of Hazardous Mate-rials, 2009; 164: 1286-1292.

18. Fahmy, R. Mix, A. Schönhals, J. Friedrich; Plasma Chemistry and Plasma Processing, 2011; 31: 477-498.

19. K. Chakarova, S. Ando-nova, L. Dimitrov, K. Hadj-iivanov; Microporous and Mesoporous Materials, 2016; 220: 188-197.

20. Y. M. Liew, H. Kamarudin, A. M. M. Al Bakri, M. Luqman, I. K. Nizar, C. M. Ruzaidi, C. Y. Heah; Cons-truction and Building Mate-rials, 2012; 30: 794-802.

21. Y. P. de Pena, W. Rondón; American Journal of Analy-tical Chemistry, 2013; 4: 387-397.

22. P. J. Launer, B. Arkles, Reprinted from Silicon Compounds: Silanes and Silicones (Eds.), Gelest, Inc Morrisville, PA., 2013.

23. Fahmy, R. Mix, A. Schönhals, J. Friedrich, PlasmaChemistryand Plasma Processing, 2012; 32: 767-780.

24. Fahmy, J. Friedrich; Journal of Adhesion Science and Technology, 2013; 27: 324-338.

25. Saravanan, V. Brindha, S. J. Krishnan; Advances of Bioinformatics, 2011; 2: 193-196.

26. T. Frising, P. Leflaive; Microporous and Mesop-orous Materials, 2008; 114: 27-63.

27. Y. Wen, C. Shen, Y. Ni, S. Tong, F. Yu; Journal of Hazardous Materials, 2012; 201: 162-169.

28. W. Shen, Z. Li, Y. Liu; Recent Patents of Chemical Engineering, 2008; 1: 27-40.

29. Balandis, A. Traidaraite; Materials Science, 2013; 19(3): 319-325.

30. R. L. Hartman, H. S. Fogler; Langmuir, 2007; 23: 5477-5484.

31. Saka, Ö. Şahin, M. M. Küçük; International Journal of Environmental Techn-ology, 2012; 9: 379–394.

32. Ö. Yavuz, C. Saka; Applied Clay Science, 2013; 85: 96–102.